Design of Mixed PDMS-mPEG Slippery Covalently Attached Liquid-like Surfaces

Jae Hyung Cho,[†,‡] Isaac J. Gresham,[†] Anthony Katselas,[†] Glen McHale,[¶] and Chiara Neto[*,†]

†*School of Chemistry and the University of Sydney Nano Institute, The University of Sydney, Sydney, 2006, NSW, Australia*

‡*Synthesis Research, Central Research Institute, KCC Corporation, 17-3, Mabuk-ro 240beon-gil, Giheung-gu, Yongin-si, Gyeonggi-do, 16891, Republic of Korea*

¶*Institute for Multiscale Thermofluids, School of Engineering, The University of Edinburgh, Edinburgh, EH9 3FB, U.K.*

E-mail: chiara.neto@sydney.edu.au

Abstract

Low droplet friction is desirable in many circumstances in which liquids interact with solid surfaces. This study explores the fabrication of surface-grafted, liquid-like layers with ultra-low static droplet friction, made from a mixture of hydrophobic polydimethylsiloxane (PDMS) and hydrophilic methoxy polyethylene glycol (mPEG). These mixed layers are prepared via a two-step spin coating process, in which reactive ethanol solutions are applied to the surface in sequence. Both polymers are liquid at room temperature and, when mixed, lead to slippery layers with contact angle that can be tuned from that of pure PDMS to that of pure mPEG. A contact angle hysteresis of $0.9 \pm 0.3^\circ$ was obtained on mPEG_{9-12} layers. This is the lowest hysteresis reported for any hydrophilic covalently-attached liquid surface, and represents the lowest contact line friction ever observed on a solid planar surface. As the PDMS fraction in

the mixed layer increased, so too did contact angle hysteresis, reaching a maximum value of 9° at 70% PDMS, before returning to 2° for the pure PDMS layer. Atomic force microscopy mapping of the liquid layers revealed that the two polymers are fully mixed on the surface, even at high surface fraction of both components. The model by Reyssat & Quéré, devised to explain contact angle hysteresis for surface with dilute defects, explains the observed results well. This study shows that liquid-like surfaces can be achieved that are more slippery than conventional self-assembled monolayers, and share the same capacity to gradually tune surface wettability. These mixed layers are excellent model systems with which to study interfacial phenomena, such as wetting, adhesion, and friction, the interactions of proteins and cells with surfaces, and for applications, from increased heat transfer, to efficient atmospheric water capture, to anti-fouling.

Keywords: slippery surfaces, quasi-liquid surfaces, SOCAL, QLS, SCALS, contact angle hysteresis, droplet mobility

1 Introduction

Slippery covalently attached liquid-like surfaces (SCALS) are an emerging family of materials with exceptionally low static friction to droplets and with potential to enhance efficiency in many applications, such as atmospheric water capture, anti-fouling, self-cleaning, anti-icing and anti-scaling.[1,2] SCALS consist of liquid polymers that have been chemically grafted to smooth substrates.[1,3] Polydimethylsiloxane (PDMS) and short chain polyethylene glycols (PEG), in particular, 2-[methoxy(polyethyleneoxy)$_n$propyl]trimethoxysilane (mPEG), are two such liquid polymers (Figure 1a) and b)). They are covalently grafted to the surface silanol groups of silica (here the native silicon oxide layer on top of silicon wafers) through condensation reactions (Figure 1d) and f)).[1] PDMS is known for its flexibility, hydrophobicity, thermal and chemical stability and low surface tension,[4] while mPEG is valued for its

hydrophilicity, protein anti-fouling properties and biocompatibility.[5]

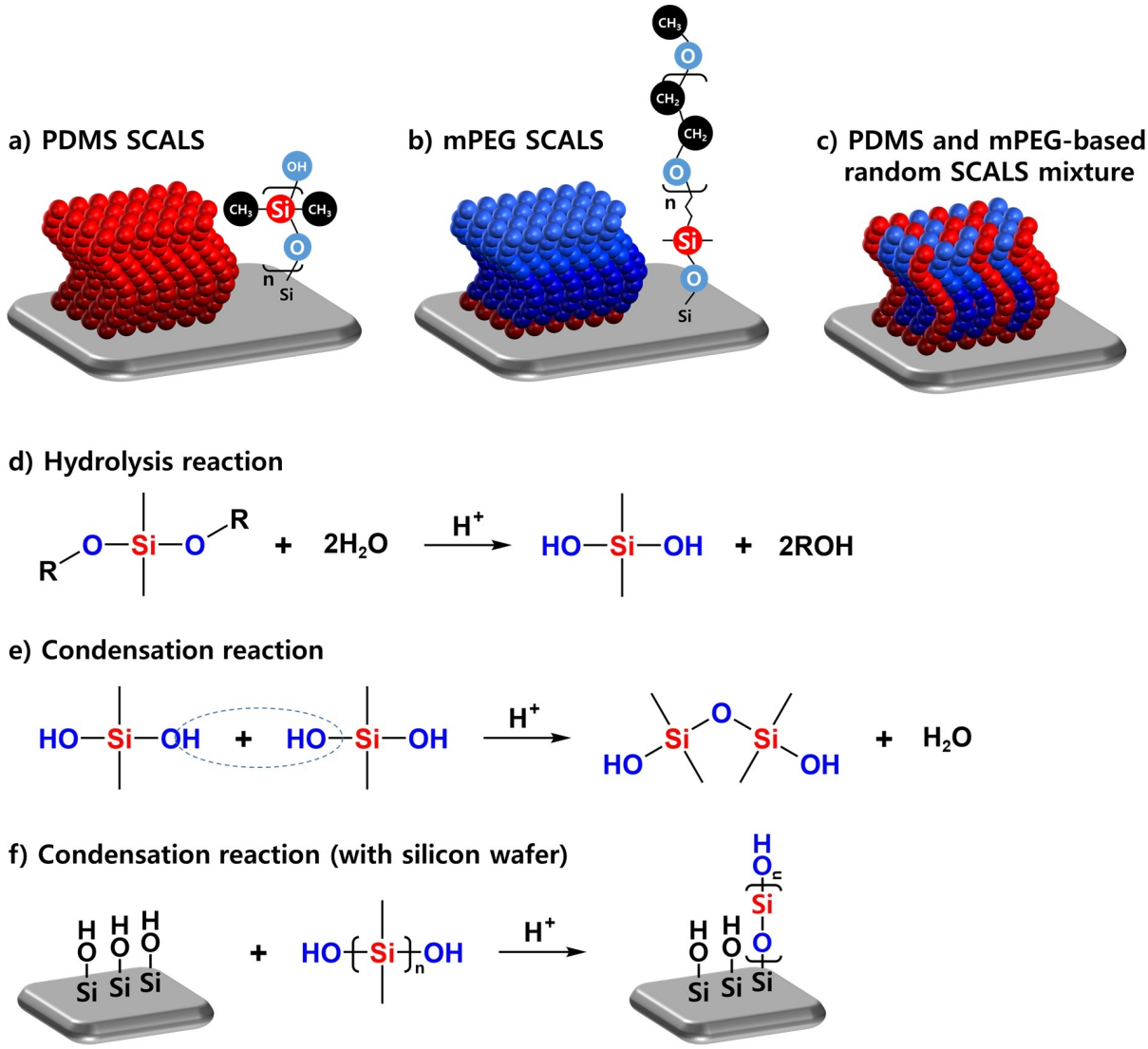

Figure 1: Schematic structure of SCALS grafted on silica surfaces: a) hydrophobic silanol-terminated PDMS SCALS, b) hydrophilic mPEG SCALS, c) possible mixed layer containing both PDMS and mPEG, in completely mixed arrangement. The length of the PDMS and mPEG chains is not necessarily the same. Grafting reactions of alkoxy silane: d) hydrolysis of alkoxy silane groups to produce silanol groups, e) condensation of silanols to produce siloxane chains, followed by f) condensation between silanols of the reactant and silanols on the silicon wafer. In both hydrolysis and condensation steps H_2O is both a reactant and product. The humidity of the environment in which the grafting reaction is conducted affects dramatically the thickness and quality of the produced layers.

Both PDMS and mPEG SCALS exhibit ultra-low droplet static friction, most readily characterized by the low contact angle hysteresis (CAH) — the difference between the

advancing and receding contact angles (ACA/RCA), measured by volume addition and withdrawal in the limit of zero contact-line velocity. CAH is an extremely sensitive measure of intermolecular interactions at the surface, and an excellent predictor of other desirable surface properties, such as anti-icing, anti-scaling and anti-fouling.[1] Grafted PEG brushes have been long known for their protein anti-fouling properties,[6,7]and recently, it has been shown that grafted layers of short chain $mPEG_{6-9}$ achieve large heat transfer enhancements and increased rate of steam and atmospheric water condensation,[8–11] compared to conventional surfaces. Despite these benefits, $mPEG_{6-9}$ is one of only two mPEG surfaces reported as slippery to droplets in the literature. The low CAH of both the PDMS and mPEG surfaces is relatively robust; hysteresis does not increase with washing with solvent or exposure to water droplets[1,10]. PDMS surfaces are stable in ambient conditions for years[12], and can withstand light abrasion, exposure to UV light, and elevated temperatures ($<150\,^{\circ}C$)[1]. mPEG surfaces are less chemically stable — PEG is known to slowly crosslink in the presence of oxygen, and mPEG surfaces are generally stored under water to slow this. However, mPEG surfaces are durable enough for experiments, for instance, the CAH of mPEG surfaces remained unchanged after 15 hours of vapor condensation[10].

The value of CAH is much more indicative of molecular uniformity than contact angle measurements;[13] for example, a surface with CAH = 1° exerts half the static friction force on a droplet than one with a similar contact angle but a CAH = 2°.[14] SCALS exhibit exceptionally low CAH, with values as low as 1° for PDMS[15,16] and 3°[9] for mPEG SCALS. These CAH values correspond to much lower droplet friction than alkane self-assembled monolayers, including those considered slippery.[17] Gresham et al. showed that the most slippery PDMS SCALS could be obtained at a reduced grafting density of $\Sigma \approx 2$, i.e. when the PDMS brush layer was sufficiently dense to uniformly coat the silicon substrate, but not too thick as to exhibit deformation and waviness which pin the droplet contact line.[18] This optimal value of reduced grafting density corresponded to a specific layer thickness of 3.5 nm, which is consistent with those reported by other groups.[2,19]

While it is clear that layers need to be homogeneous and dense to achieve SCALS performance, the minimum size of a defect that will induce an increase in CAH within these layers is not known. Given that both the hydrophilic and hydrophobic chains are liquid-like, can they be mixed, and produce a uniform layer that still retains a low CAH? PDMS SCALS containing mostly methyl-terminated chains exhibit an ACA of 107° and those containing also silanol-terminated chains exhibit a lower ACA of 104°,[3,15,16] but they both have similarly low CAH.[16,20] This is surprising, as the presence of hydrophilic defects in the silanol-terminated case would be expected to increase CAH.[21]. It appears that a minimum defect size is required to pin the contact line in liquid-like coatings; below this size, the defect can be hidden by thermal motion in the layer, and only influences *dynamic* CAH.[16,22] However, the minimum size of this type of defect is unclear.

'Mixed SCALS', i.e. with intermediate contact angle values between that of PDMS (104°) and that of mPEG (40°) have not been yet prepared, even when PDMS and mPEG were purportedly patterned on the same surface.[23] Yet the ability to control the composition and the structure of mixed layers could make SCALS excellent systems for the study of interfacial phenomena such as wetting, adhesion, friction, and protein and cell adsorption, as has been done with conventional self-assembled monolayers.[17,24–27]

The reproducible synthesis of pure SCALS is not straightforward, requiring fine control of environmental humidity, cleanliness and density of silanols groups on the solid surface.[1] Preparation of the mixed PDMS-mPEG system is even more challenging as the reaction conditions used to achieve the SCALS of the PDMS and mPEG are drastically different. The synthesis of highly slippery mPEG SCALS is slow, taking over 18 hours at room temperature,[10] while that of dimethoxydimethylsilane (a PDMS monomer) can be fast, reacting over only tens of seconds at room temperature.[15] Given the low miscibility of PDMS and mPEG, mixed SCALS could be expected to phase-separate into islands of each molecule, as has been observed for some mixed self-assembled monolayers.[28–31]

In this study, a 2-step spin coating method was developed that allowed the preparation

of mixed monolayers of PDMS and mPEG on silicon wafers. Spin coating improves reproducibility by enabling precise control over both the deposited film thickness and relative humidity, relative to drop casting and dip coating approaches previously used.[15,22] This is because, in preparing SCALS from a solution of a reactive species, the precise rate of reaction depends on both the evaporation of solvent from the film, and the absorption of water into the film from the atmosphere. The proposed method uses non-toxic solvents (ethanol and isopropanol) rather than commonly used toluene. The method produces homogeneous SCALS with low CAH of $\approx 1^\circ$ for $mPEG_{9-12}$ and $\approx 2^\circ$ for PDMS. For mixed SCALS, the ACA can be varied continuously between that of mPEG and PDMS. AFM studies of both topography and adhesion force reveal that mPEG and PDMS chains are uniformly distributed within these mixed layers, with no patterns visible. In the mixed system, CAH increases as a 50:50 mixture is approached.

2 Results and Discussion

In this work, a protocol alternative to the commonly used method, namely immersion in toluene solutions, was devised to produce mPEG layers, using three chain lengths; the method uses non-toxic solvents, allows better reproducibility of the layers and, using $mPEG_{9-12}$, produces the lowest CAH value of any mPEG previously prepared.

2.1 Synthesis and properties of mPEG SCALS

Firstly, three different synthetic protocols for mPEG slippery layers were tested: drop casting and spin coating of ethanol solutions, and the established protocol of immersion in toluene solutions (included here as a baseline).[8,9] Three different mPEG chain length values were tested, $mPEG_{6-9}$, $mPEG_{9-12}$ and $mPEG_{21-24}$. Details are provided in the Materials Section.

In immersion coating, the silicon wafer substrate was immersed in a toluene solution in a sealed N_2-purged Atmosbag for 18 hours. Immersion using the $mPEG_{6-9}$ solution resulted

in the desired layer of thickness 1.5 nm, while $mPEG_{9-12}$ and $mPEG_{21-24}$ resulted in thinner layers (0.4 nm for both), indicating a low grafting density (Figure 2a). This low grafting density is attributed to the increase in polymer chain length, which reduces solubility.

Investigations of spin-coating approaches for mPEG functionalization revealed that alcohols (ethanol, EtOH or isopropanol, IPA) were a superior solvent. In alcohols mPEGs are more soluble and more water is present, which is required to hydrolyze silane endgroups, further enhancing the grafting process. Spin coating and drop casting of ethanol solutions consistently produced lower CAH values than immersion in toluene. Drop casting, in which the polymer solution was dropped onto the substrate and allowed to evaporate over 15 minutes (inspired by the method of Wang and McCarthy[15]), resulted in higher CAH values than spin coating. The centrifugal force in spin coating promoted even spreading of the solution and rapid solvent evaporation, leading to the formation of homogeneous thin layers.

As shown in Figure 2a), spin coating the solution produced the lowest CAH values: 1° for $mPEG_{9-12}$, 3° for $mPEG_{21-24}$, and 4° for $mPEG_{6-9}$. In contrast, drop casting under similar conditions resulted in higher CAH values. As shown in Figure 2a), regardless of chain length, spin coating consistently yielded lower CAH values compared to drop casting and immersion methods. Based on these results, spin coating was selected as the preferred deposition method and optimized.

Table 1 details the synthetic conditions tested to prepare pure mPEG SCALS using $mPEG_{6-9}$ and $mPEG_{9-12}$. Thermal curing was required to obtain layer thickness above 1 nm (needed for slippery layers[10]), irrespective of the catalyst used. To increase the length of the grafted chains, two thermal curing steps were tested. In a pre-curing step, the reactant solution was heated at 50 °C for 30 min, 3 hours and 20 hours, before spin coating, but this treatment did not affect the grafted thickness. On the other hand, when a post-curing step was added (after spin coating and before washing), by heating the mPEG surface for 20 hours at 50 °C, the resulting layers increased in thickness and became extremely slippery. The thickness increased to an average of 1.9 ± 0.1 nm, and the CAH decreased to an average

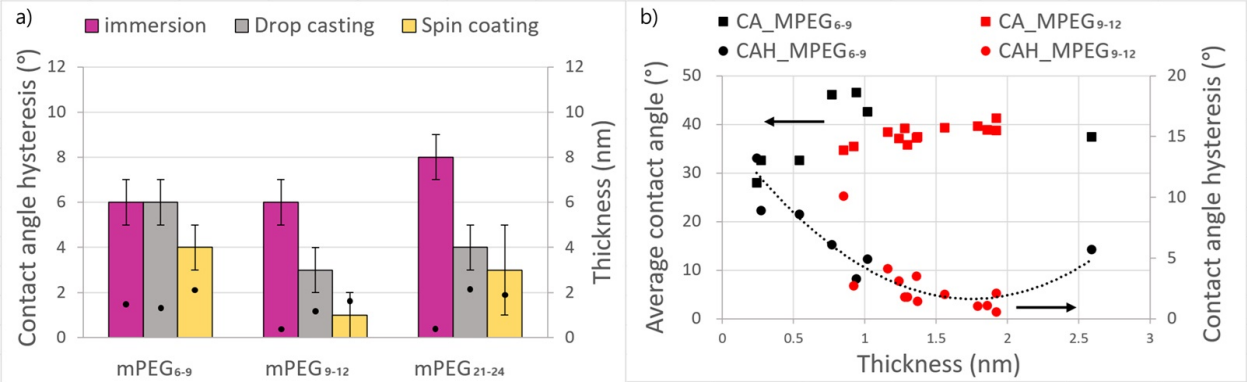

Figure 2: Screening of deposition methods for mPEG SCALS. a) CAH (bars, left axis) and thickness (dots, right axis) of mPEG layers prepared by immersion in toluene solution (purple bars), by drop casting (gray bars) and spin coating (yellow bars). The error on the thickness values was ±0.1 nm. b) Average contact angle (CA, squares) and contact angle hysteresis (CAH, circles) obtained on mPEG SCALS prepared by spin coating during the optimization of reaction conditions. Only the two more promising mPEG sources, $mPEG_{6-9}$ (black) and $mPEG_{9-12}$ (red), were characterized further. The dotted line is a guide to the eye.

of 0.9 ± 0.3° (roll-off angle of 3.3° for a 10 µL droplet). This corresponds to a normalized friction of between 0.7 (from CAH) and 1.1 μN/mm (from roll-off), the lowest ever observed for a planar solid surface.[17]

Table 1: Reaction conditions and physical properties of pure mPEG SCALS prepared by spin coating solutions as shown. Layer thickness measured by ellipsometry, advancing (ACA) and receding (RCA) contact angle and contact angle hysteresis (CAH) are shown. Acetic acid was mixed with the solvent and Milli-Q water, primarily to adjust the pH to 4. For example, 95 wt% of solvent (by weight) and 5 wt% of Milli-Q water were thoroughly mixed and adjusted to pH 4 adding acetic acid (AA). The conditions used for the most slippery layers are in bold. In all cases, RH was controlled below 10% during synthesis, and the spin coating was performed at 2,000 rpm for 60 s.

Components				Pre-curing		Post-curing		Property			
Solvent (g)	$mPEG_{6-9}$ (g)	$mPEG_{9-12}$ (g)	H_2SO_4 (g)	Temp.(°C)	Time	Temp.(°C)	Time	Thickness(nm)	ACA(°)	RCA(°)	CAH(°)
IPA	0.1	-	8.0×10^{-5}	-	-	-	-	0.2	34.6	21.4	13.2
1.0	-	0.1	8.0×10^{-5}	-	-	-	-	0.9	39.7	29.6	10.1
EtOH(95)	0.05	-	-	-	-	-	-	0.8	49.2	43.1	6.1
$+H_2O$(5)	-	0.05	-	50	30 min	-	-	0.9	48.2	44.9	3.3
→ pH4 (AA)	-	0.05	-	50	3 h	-	-	1.0	45.0	40.1	4.9
	-	0.05	-	50	20 h	-	-	0.5	36.9	28.3	8.6
1.0	-	**0.05**	-	-	-	**50**	**20**	**1.9 ± 0.1**	**40.4 ± 1.1**	**39.5 ± 1.4**	**0.9 ± 0.3**

In an attempt to reduce the post-curing time, the curing temperature was increased from 50 to 90 °C (Table S3) but the CAH increased significantly to 9.1° despite the thickness

remaining constant. It is known that mPEG cures differently with curing conditions:[32] at lower temperature, condensation reactions proceed more slowly, leading to linear or less cross-linked structures. At higher temperature more cross-linking occurs, leading to denser network structures.[33]

All data from the mPEG optimization experiments is presented in Figure 2b). The $mPEG_{9-12}$ SCALS with a thickness close to 2 nm showed the lowest CAH, with a minimum of 0.9°, which is the lowest CAH value yet reported for mPEG layers. This minimum in CAH occurred at the point where ACA for the $mPEG_{9-12}$ reached the value of 40°. The topography of the mPEG SCALS was smooth, uniform and featureless, with an RMS roughness close to the value measured on plain silicon wafers (≈ 0.22 nm), as shown in Figure S1.

2.2 Synthesis and properties of PDMS SCALS

The spin coating method was adopted to prepare pure PDMS SCALS, using three sources of PDMS: silanol-terminated PDMS (OH-PDMS), chlorine-terminated PDMS (Cl-PDMS) and monomers of dimethoxy dimethylsilane (DMDMS). Unless specified, throughout the paper results shown for PDMS layers were obtained by grafting OH-PDMS. Table 2 shows the results of varying the concentration of catalyst H_2SO_4 in the reactant mixture, to prepare PDMS SCALS using OH-PDMS as a source. When layers were obtained without control over RH, poor reproducibility in layer thickness, contact angle and CAH was obtained (Table S2). In contrast, when RH was controlled, the results were reproducible. The amount of adsorbed water on the silicon wafer was reduced by pre-heating the substrates at 150 °C for 1 min just before spin coating, and ambient humidity was reduced by purging the spin coater chamber with N_2 until RH $< 10\%$. With these changes, the trends in layer thickness with catalyst concentration became consistent, as shown in Table 2. The most slippery PDMS SCALS, with CAH of $2.1 \pm 0.5°$, and roll-off angle of 4.6° (for a 10 µL droplet), were obtained using OH-PDMS as a source, for a layer thickness of 2.9 ± 0.1 nm using 8×10^{-5} g of H_2SO_4.

Figure 3 highlights the relationship between layer thickness, average contact angle (CA =

Table 2: Optimization of reaction conditions and physical properties of PDMS SCALS prepared by spin coating OH-PDMS under humidity control (RH $< 10\%$). Layer thickness measured by ellipsometry, advancing (ACA) and receding (RCA) contact angle and contact angle hysteresis (CAH) are shown. Errors correspond to standard deviation on the mean. When no error is shown, only 1 repeat was conducted, appropriate for this screening study. The conditions obtained for the most slippery layers are in bold. The spin coating was performed for 60 s.

solvent (g)	SCALS source (g)	catalyst (g)	Coating Condition		Physical Properties			
IPA	OH-PDMS	H_2SO_4	Temp. (°C)	RPM	thickness (nm)	ACA (°)	RCA (°)	CAH (°)
1.0	0.1	4.8×10^{-5}	19.5	2,000	(1.0 ± 0.1)	(100.1 ± 0.6)	(90.9 ± 2.4)	(9.2 ± 3.0)
		8.0×10^{-5}	22.7	**2,000**	**2.9 ± 0.1**	**105.5 ± 1.5**	**103.4 ± 2.0**	**2.1 ± 0.5**
			22.7	3,000	3.1	104.9	102.8	2.1
		1.2×10^{-4}	22.7	1,000	4.4	107.7	103.6	4.1
			22.7	2,000	4.5	108.3	103.2	5.1

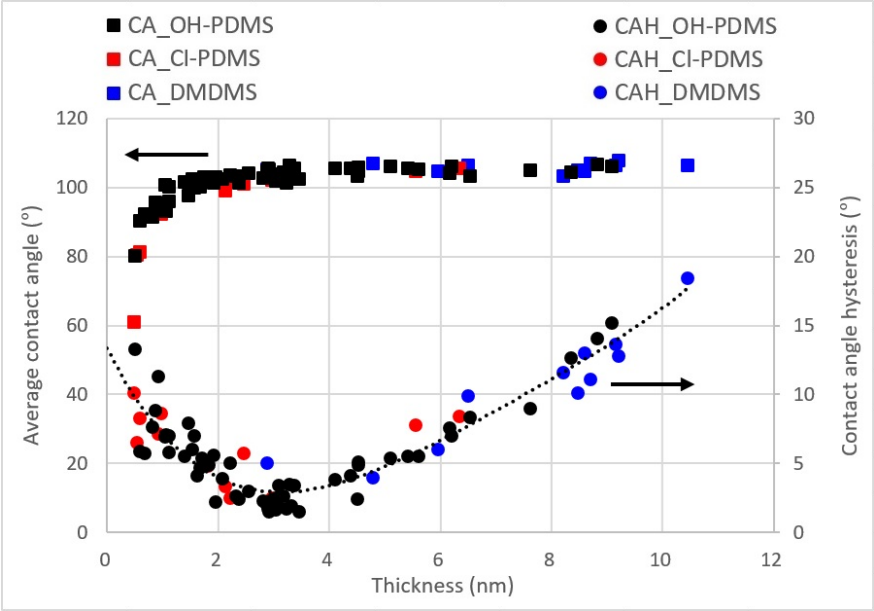

Figure 3: Average contact angle (CA, squares) and contact angle hysteresis (CAH, circles) of water on PDMS layers prepared during optimization of the spin coating process. Various PDMS sources, including OH-PDMS (black), Cl-PDMS (red), and DMDMS (blue), were used to create the PDMS layer. Each data point is the average of two measurements taken on the same surface. The line is a guide to the eye and represents a parabolic fit. PDMS layers with thickness = 20 nm could also be obtained, but they exhibited CAH = 28°.

(ACA+RCA)/2), and CAH for PDMS SCALS obtained from all three sources. A minimum in CAH at intermediate layer thickness (around 3.5 nm) has been recently explained as due to a specific reduced grafting density that balances substrate coverage and layer smoothness.[3,18] This trend is consistent regardless of the functional group or molecular weight of the SCALS

source. The lowest value of CAH measured on a single wafer was 1.7°, with a corresponding thickness of 2.9 nm. Prior work indicates that this optimal layer is comprised of chains of between 20 and 40 repeat units, corresponding to a contour length of between 6.5 and 13 nm.[3] This minimum in CAH occurred at the point where the CA reached the value of 106.5°. Below thickness of 3 nm, SCALS CA decreased sharply, because the PDMS did not entirely cover the silicon substrate. For layers thicker than 3 nm, the CA was reasonably constant while the ACA gradually increased with thickness (corresponding to increasing CAH). All three PDMS sources lead to approximately the same CA, and exhibited the same trend in CAH with layer thickness, as evidenced in Figure 3. These trends indicate that the lowest CAH SCALS have the minimum thickness required to suppress interaction between the substrate and the silica substrate; for a more detailed explanation see the work of Rasera et al.[18] It was possible with this approach to synthesize much thicker PDMS layers; for example, a layer 20 nm thick with CAH = 28° was prepared by using 4.0 $\times 10^{-4}$ g of H_2SO_4 catalyst, followed by post-curing at room temperature for 19 hours.

The topography and thickness of PDMS SCALS were measured by atomic force microscopy (AFM) meniscus force maps (MFM), and are shown in Figure 4. More details are shown in the Methods Section. The first row a)-c) displays the topography of each surface, taken from the hard-contact location. The topography of the plain PDMS SCALS is as smooth and featureless as that of the plain silicon wafer substrates, with an RMS roughness of $r_q \approx 0.2$ nm. The second row d)-f) displays maps of the thickness of the liquid layer on the surface, and is generated by mapping the point at which the approaching AFM tip jumps into contact with the film, due to the meniscus capillary attraction.[34] A liquid layer of finite thickness is detected on the plain silicon wafer (median thickness value of 2 nm), caused by a water layer present on all surfaces exposed to the atmosphere.[35] A thicker layer due to the polymer is detected on the PDMS SCALS: on the 2.9 nm thick PDMS layer (as measured by ellipsometry), the average jump-in value is 3.7 nm, and on the 6.4 nm thick layer the average jump-in value is 10 nm. MFM overestimates the layer thickness by 2-3 nm relative

to ellipsometry because of both the presence of a water film on the surface and deformation of the PDMS layer due to attractive van der Waals forces with the tip.[34] The roughness observed on thicker PDMS layers was much higher than that of thinner layers (Figure 4f), due to the emergence of waviness in the layer, an effect reproduced in recent molecular dynamics simulations:[18] thicker layers consist of chains of higher molecular weight, and higher polydispersity. Rasera et al. showed that polydisperse chains lead to the emergence of surface waviness in the layers, due to the lateral and vertical microphase separation of the longer chains into bumps.[18]

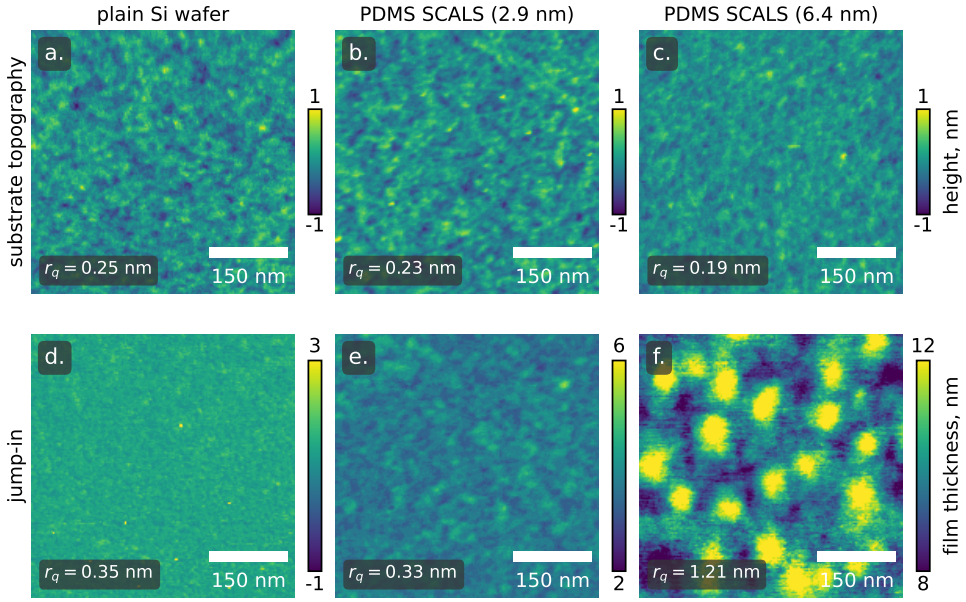

Figure 4: Maps of a)-c) topography and d)-f) jump-in point (approximately equal to liquid layer thickness) obtained by MFM on a), d) plain silicon wafer, b), e) 2.9 nm thick PDMS SCALS (prepared from silanol-terminated PDMS), and c), f) 6.4 nm thick PDMS layers. PDMS layers much thicker than 3.5 nm are no longer slippery. The root-mean squared roughness (r_q) is shown in each panel.

2.3 Attempted synthesis of mixed PDMS-mPEG layers by spin coating a single solution

As both grafted PDMS and mPEG chains produce liquid-like layers on their own, it was natural to wonder whether mixed layers containing both types of chains would still be liquid-like. Mixed or patchy self-assembled monolayers are routinely prepared from mixed solutions of hydrophilic and hydrophobic molecules, and allow to test theories on the effect of defects or domain formation on CAH.[26,28–31] A spin coating procedure to prepare mixed layers from a single ethanol solution of PDMS and mPEG was optimized and is shown in Section S2. Grafting of a mixed SCALS from a single solution was not possible using the chosen method, at any mixing ratio tested. While layers of low CAH could be prepared, the ACA and thickness remained low, matching those of plain mPEG SCALS, as shown in Table 3. This can be explained with a first rapid physisorption step, whereby mPEG physisorbed strongly to the hydrophilic Si wafer, blocking access to the PDMS chains, which were more hydrophobic and slower to reach the surface. In a second slower step, likely mPEG chains reacted with the silicon surface, leading to stable, slippery SCALS with low PDMS content.

Table 3: Unsuccessful preparation of mixed SCALS by spin coating a single ethanol solution of PDMS and mPEG. Mixing ratios of PDMS and mPEG solutions are shown, along with the corresponding thickness, advancing contact angle (ACA), receding contact angle (RCA), and contact angle hysteresis (CAH). The values of ACA and RCA indicate that only mPEG was effectively grafted.

ratio		property			
PDMS	mPEG	thickness(nm)	ACA(°)	RCA(°)	CAH(°)
10	0	2.08	104.3	100.4	3.9
7	3	1.16	38.6	35.0	3.6
5	5	1.05	38.2	35.4	2.8
3	7	1.16	38.4	35.3	3.1
0	10	1.37	38.2	36.7	1.4

2.4 Synthesis of mixed PDMS-mPEG layers using a 2-step spin coating method

To fabricate mixed PDMS-mPEG SCALS, a 2-step grafting approach was introduced, requiring two successive spin coating steps. The procedure is schematically shown in Figure 5a), and further described in the Methods Section, Table S5 and section S3. First, a droplet of an IPA solution of OH-PDMS was dispensed on the silicon wafer which was already spinning at 2,000 RPM; then, after reaction times varying between 5 s - 120 s, the ethanol solution of mPEG was dispensed on the surface, which effectively replaced the liquid PDMS on the surface and started the mPEG grafting reaction (Figure S3). Although the surface tension of silicone oil is lower than than of mPEG (nominal values $\gamma_{PDMS} \approx 21$ mN/m and $\gamma_{PEG} \approx 44$ mN/m), the strong hydrogen bonding of mPEG, as well as the mechanical action due to the added volume, acts to favor mPEG replacing PDMS. PDMS grafted rapidly to the silicon wafer surface, but reaction times shorter than 60 s created an incomplete or low grafting density PDMS layer on the silicon wafer. Presumably, the molecular weight of PDMS produced by these reactions is lower than those observed in the pure-PDMS case, where longer reaction times were used (Gresham et al.[3] found that a similar approach produced PDMS chains with twenty repeat units); that is, with contour length comparable to the grafted mPEG (PDMS of ten repeat units is expected to have the same contour length as $mPEG_{9-12}$). This low density PDMS layer was back-filled with mPEG in the second spin coating step, and after the spin coating, the mixed layer was allowed to react for 20 hours at 50 °C, as shown in Table 4. The results of this successful 2-step process are shown in Figure 5b) and in Figure S4.

The average contact angle in Figure 5b) and Table 4 increased as the PDMS reaction time increased; the mPEG reaction time was kept the same in all cases. The measured contact angle of pure mPEG SCALS was 40° and that of pure silanol-terminated PDMS SCALS was 104°. When PDMS was allowed to react on the silicon wafer for the shortest time (5 s) before allowing the mPEG to react, the CA obtained was (within error) that of pure mPEG

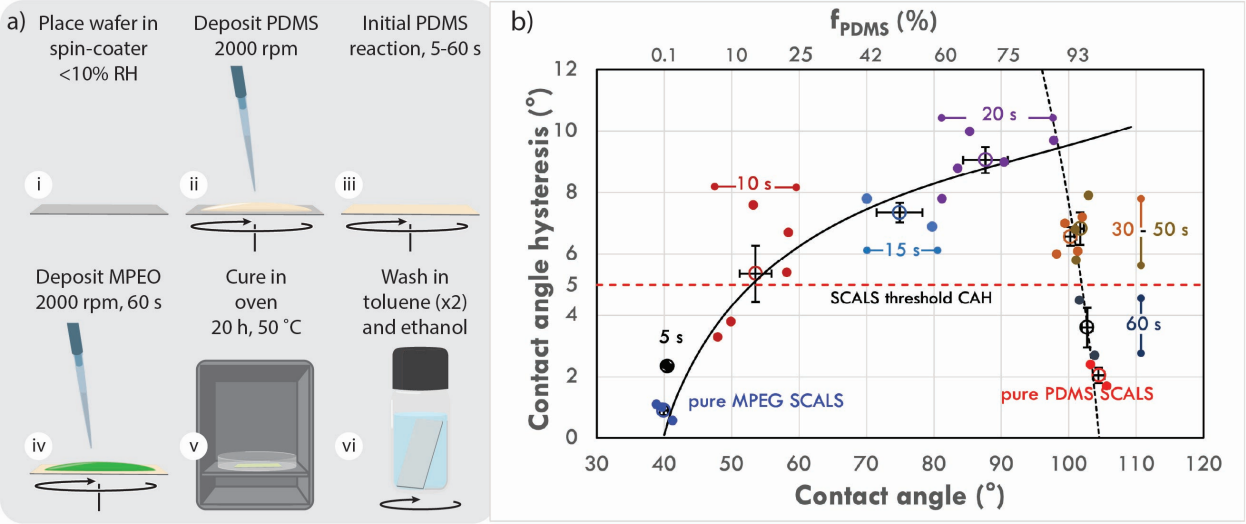

Figure 5: a) Schematic of the procedure to prepare mixed SCALS layers using the 2-step spin coating method. b) Contact angle hysteresis vs average contact angle (CA = (ACA+RCA)/2) and versus PDMS surface fraction (upper x-axis, obtained through the Cassie Equation[36]) for mixed PDMS-mPEG layers. The red symbol represents the value for a pure PDMS SCALS, and the blue symbol that for a pure mPEG SCALS. The labels and colors on the graph identify PDMS reaction times. The red dashed line identifies the threshold CAH value for a layer to be defined as SCALS. Individual each data points are shown as smaller symbols with no error bar. The corresponding averages are shown with error bar. The solid line is the fit of the Reyssat & Quéré model (Equation 2),[37] using a=0.58 with PDMS regarded as defects on a mPEG surface; the dashed black line is the same model using a = 1.9 with mPEG regarded as defects on a PDMS surface.

SCALS, but the CAH increased from 0.9 to 2.4°. The increase in CAH was due to the presence of defects in the mPEG layer, i.e. the low but finite surface area fraction of grafted PDMS chains, $f_{PDMS} \approx 0.6\%$, based on a Cassie model of biphilic surface chemistry.[36,38] At 10 s PDMS reaction time, both CA and CAH increased, indicating that the PDMS was grafted at higher coverage, $f_{PDMS} \approx 17\%$, but still as an incomplete layer, so the mPEG layer (applied subsequently) covered the remaining exposed area of the silicon wafer. The CAH of the mixed layers increased to a maximum of 9°, corresponding to $f_{PDMS} \approx 71\%$, after which it began to decline again. At 30 s of PDMS reaction, the CAH was lower, suggesting that PDMS was well coated, $f_{PDMS} \approx 93\%$, allowing only a small coverage of mPEG on the Si wafer. As shown in Table 4, through gradual increase in PDMS reaction time, mixed layers of hydrophilic mPEG and hydrophobic PDMS were fabricated. Setting CAH = 5°

Table 4: Properties of mixed PDMS/mPEG SCALS prepared through the 2-step spin coating process: layer thickness, advancing and receding contact angle (ACA/RCA), average contact angle (CA: average of advancing and receding contact angle), and contact angle hysteresis (CAH) versus PDMS reaction (spinning) time on the surface. A value of 'none' under PDMS reaction time corresponds to a pure mPEG SCALS. The PDMS surface area fraction (f_{PDMS}) was calculated using the Cassie Equation.[36]

PDMS reaction time	none (mPEG)	5 s	10 s	15 s	20 s	30 s
thickness (nm)	1.9 ± 0.1	1.6 ± 0.0	1.6 ± 0.3	1.5 ± 0.3	1.3 ± 0.1	1.4 ± 0.2
ACA (°)	40.4 ± 1.1	41.7 ± 0.4	56.2 ± 5.4	78.6 ± 6.5	92.2 ± 6.9	103.5 ± 1.9
RCA (°)	39.5 ± 1.4	39.3 ± 0.4	50.9 ± 4.2	71.3 ± 7.1	83.1 ± 6.3	97.0 ± 1.6
CA (°)	39.9 ± 1.2	40.5 ± 0.4	53.5 ± 4.8	74.9 ± 6.8	87.6 ± 6.6	100.2 ± 1.8
CAH (°)	0.9 ± 0.3	2.4 ± 0.1	5.4 ± 1.8	7.4 ± 0.6	9.1 ± 0.9	6.6 ± 0.6
f_{PDMS}(%)	0	0.6	17	50	71	93
PDMS reaction time	50 s	60 s	90 s	120 s	PDMS	
thickness (nm)	1.9 ± 0.2	2.9 ± 0.2	4.9	8.6	2.9 ± 0.1	
ACA (°)	105.1 ± 1.6	104.6 ± 0.9	108.0	109.4	105.5 ± 1.5	
RCA (°)	98.2 ± 0.8	103.4 ± 2.0	102.4	100.5	103.4 ± 2.0	
CA (°)	101.7 ± 1.1	102.7 ± 1.6	105.2	105.0	104.4 ± 1.7	
CAH (°)	6.8 ± 1.1	3.6 ± 1.3	5.6	8.9	2.1 ± 0.5	
f_{PDMS}(%)	95	97	100	100	100	

as the threshold for SCALS behavior, at 5 s and 60 s PDMS reaction time, corresponding to 0.6% and 97% of PDMS respectively, SCALS properties could be reproduced in a mixed PDMS-mPEG layer. For other values of mixing ratios, the layers had CAH $\leq 10°$, superior to even the most slippery alkane self-assembled monolayers (see Figure S6 for a comparison with recent literature).[17] The gradual change in CA and CAH with the gradual change of PDMS reaction time confirmed that both PDMS and mPEG chains were present on the surface at the contact line, as expected based on previous work on biphilic surfaces.[39]

To quantitatively model these results, first the average contact angle values measured were used in the Cassie model,[36] $\cos\theta_{\mathrm{ave}} = f_{\mathrm{PDMS}}\cos\theta_{\mathrm{PDMS}} + f_{\mathrm{mPEG}}\cos\theta_{\mathrm{mPEG}}$, with PDMS and mPEG contact angle values of $\theta_{\mathrm{mPEG}} = 39.9°$ and $\theta_{\mathrm{PDMS}} = 104.4°$, to calculate surface fractions, f_{PDMS} and $f_{\mathrm{mPEG}} = 1 - f_{\mathrm{PDMS}}$ (Table 4). Starting with a mPEG dominated surface, PDMS was assumed to provide a set of strong, but dilute, defects following the model of Reyssat & Quéré,[37] which was derived from the work of Joanny & de Gennes.[40] In their

model the pinning force per unit length of contact line normalized by surface tension is

$$(\cos\theta_{\mathrm{r}} - \cos\theta_{\mathrm{a}}) \approx \frac{a\ f_{\mathrm{D}}}{4} ln(\frac{\pi}{f_{\mathrm{D}}}) \tag{1}$$

where f_D is the surface area fraction covered by defects and a is a parameter representing the distortion of the contact line. In their case of a superhydrophobic surface, the zero-hysteresis defect-free surface was the air and the defects were the hydrophobic circular micropillars arranged in a square lattice. Their fitting to their data gave $a = 3.8$ compared to an expectation for their geometry of $a \approx 2$. Their model (Equation 1) can be rewritten using the CAH and average contact angle (θ_{ave} = CA) as:

$$\mathrm{CAH} \approx \frac{a\ f_{\mathrm{D}}}{4\ \sin\theta_{\mathrm{ave}}} \ln(\frac{\pi}{f_{\mathrm{D}}}) \tag{2}$$

This model was fitted to the data for the mixed layer using $a = 0.58 \pm 0.05$ for the data in which PDMS chains are regarded as defects in a mPEG surface; the fit is shown as the solid curve in Figure 5b). Similarly, fitting this model to the data for the mixed layer using $a = 1.9 \pm 0.3$ for the data with mPEG regarded as the defects within a PDMS surface gives the dotted curve in Figure 5b). These two curves appear to describe the trends in the observed data.

The Reyssat & Quéré model (Equation 2) seems to describe correctly the contact angle hysteresis of a mPEG surface with over 50% surface coverage of PDMS defects, thereby extending beyond the dilute regime for which it was proposed.[37] For the PDMS defects within the mPEG surface, our fitted value $a = 0.58$, compared to the Reyssat & Quéré fitted value of $a = 3.8$, indicates that the PDMS defects are 6.6 times weaker than the micropillars in their superhydrophobic surface. For the mPEG defects within PDMS SCALS, the fitted value of $a = 1.9$ is half that used by Reyssat & Quéré. This means that in the mixed PDMS/mPEG layers the contact line motion is less sensitive to the presence of defects than the superhydrophobic surface was to the perfluoropolymer-coated micropillars as defects.

AFM MFM analysis was performed to simultaneously map the surface topography and the distribution of adhesive forces on the surfaces of pure mPEG, pure PDMS and mixed 2-step layers, as shown in Figure 6. The topography of the mixed systems was as smooth ($r_q \approx 0.2$) and featureless as that of the underlying silicon wafers and as the pure PDMS and pure mPEG layers, indicating that the grafting reactions progressed to produce similarly uniform layers.

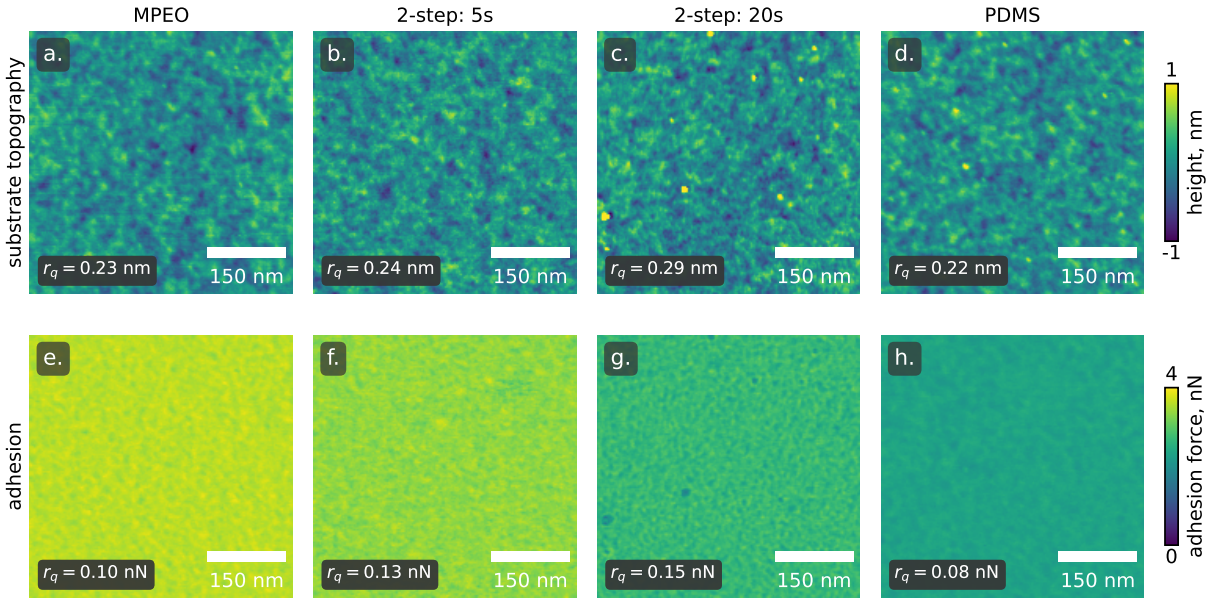

Figure 6: Representative maps of a)-d) topography and e)-h) adhesion maps obtained by MFM for the prepared mPEG, PDMS-mPEG, and PDMS layers. a) and e) pure mPEG SCALS, b) and f) mixed SCALS with 0.6% PDMS (reaction time of 5 s), c) and g) mixed SCALS with 71% PDMS (20 s), and d) and h) pure PDMS SCALS. All maps share the same scale bars. All surfaces had similar topography, with RMS roughness comparable to a silicon wafer (r_q value shown). Adhesion maps reveal a gradual decrease in adhesion, in order mPEG > PDMS1%-mPEG99% > PDMS71%-mPEG29% > PDMS, as expected based on the gradually increasing contact angle. The homogeneous adhesion maps of the mixed layers indicate that PDMS and mPEG were well mixed in the grafted layers; domains with size above the resolution of the AFM tip (≈10 nm) were not seen.

The adhesion maps were used to relate observed contrast to the chemical interaction between the hydrophilic (silicon oxide) AFM tip and regions of the sample surface. Regions of hydrophilic nature, such as silica and mPEG, are expected to show higher adhesion values than the hydrophobic PDMS ones, due to higher hydrogen bonding interactions. Figure 6e)-

h) reveal indeed that higher adhesion was measured on pure mPEG layers (yellow color corresponding to 4 nN) compared to the pure PDMS layer (adhesion around 2 nN). Mixed PDMS-mPEG layers had intermediate adhesion, as revealed by the color scale; fine dots visible in part g) are due to topographical features visible in c), likely defects. No patches in the mixed PDMS-mPEG layers were detected, meaning that defects and domains present must be smaller than the AFM tip used for the measurements (10 nm nominal radius). The absence of patches in the mixed PDMS-mPEG surfaces suggests that the hydrophilic mPEG and hydrophobic PDMS were uniformly distributed on the surface, creating a mixed surface with defect size too small to detect (as schematically shown in Figure 1c)). The absence of nanoscale or microscale phase-separated domains implies that the contact line pinning observed on the mixed SCALS is due to nanoscale defects, possibly on the scale of a few molecules. The nanoscale size of the defects might explain why the fitted a values describing the distortion of the contact line were so small. Higher (atomic) resolution AFM imaging beyond the scope of this work might be able to verify the arrangement of chains in the mixed layers.

3 Conclusions

In this study, mixed slippery liquid-like layers were fabricated using PDMS and mPEG with a 2-step spin coating process. By tuning the surface fraction of one component into a surface of the other, we fabricated slippery layers with varying density of molecular defects. Low contact angle hysteresis was achieved on the pure PDMS SCALS ($2.1 \pm 0.5^\circ$ at a thickness of 2.9 ± 0.1 nm) and on the pure mPEG SCALS ($0.9 \pm 0.3^\circ$ at a thickness of 1.9 ± 0.1 nm). The value of CAH measured on mPEG is the lowest for any mPEG surface reported so far, and corresponds to a normalized friction of between below 1.1 μN/mm, the lowest ever observed for a planar solid surface. These best-in-class coatings could be used, for example, to enhance heat transfer in condensation, even beyond the exceptional results

already reported[9]. When a single mixed solution of PDMS and mPEG was spin coated with the aim to form mixed SCALS, only mPEG SCALS formed because the rapid physisorption of mPEG prevented PDMS grafting. Using a 2-step spin coating process, mixed layers with smoothly increasing values of contact angle between 40° and 104° could be prepared, all with CAH $\leq 10°$. At short reaction time of PDMS (5 s), surface coverage was dominated by mPEG, up until 20 s, when PDMS became more prominent. During this transition, CAH reached its maximum value of 9° at 20 s and then decreased again to 3.6° at 60 s. Meanwhile, the average contact angle increased to around 105° by 60 s, the surface being entirely covered by PDMS. The mixed layers did not show any evidence of phase-separated domains of either PDMS or mPEG, so we conclude that the contact line friction increase on mixed layers is due to molecular scale heterogeneity (no defects larger than 10 nm). The model of Reyssat & Quéré fitted well the increase of contact angle hysteresis with density of defects, well beyond the dilute regime for which it was proposed. This work advances our understanding of SCALS properties and performance, and opens the way for investigations on low droplet friction coatings for use as anti-microbial, anti-icing, high heat transfer and self-cleaning coatings.

4 Materials and Methods

4.1 Materials

25 cSt OH-PDMS (silanol-terminated polydimethylsiloxane, Sigma-Aldrich, MW $\approx$ 550, corresponding to 7 repeat units), was used for most of the work. In OH-PDMS both ends of the PDMS chain bear silanol groups, and when grafted could lead to loops of silanol-terminated chains. Few samples shown in Figure 3 were prepared using Cl-PDMS (chlorine-terminated poly (dimethylsiloxane), Mn 3,000 Da corresponding to 40 repeat units, Sigma-Aldrich; both ends of the PDMS chain bear chloride groups) and DMDMS (dimethoxydimethylsilane, Sigma-Aldrich; difunctional PDMS monomer). All three approaches result in silanol-

terminated PDMS layers, as indicated by their average contact angle (103.8°), similar to 104° initially reported by Wang and McCarthy.[15]

The mPEG layers were prepared using $mPEG_{6-9}$ (2-[methoxy(polyethyleneoxy)6-9 propyl] trimethoxysilane, $M_n = 459-591$ g/mol, Fluorochem) and $mPEG_{9-12}$ (2-[methoxy(polyethylene oxy)9-12 propyl]trimethoxysilane, M_n = 591–723g/mol, Fluorochem). The two mPEG chains are expected to have a contour length of 2.1 and 2.9 nm, respectively, based on a PEG repeat unit length of 0.28 nm[41]. Some synthesis tests were also conducted with $mPEG_{21-24}$ (2-[methoxy(polyethyleneoxy)21-24propyl] trimethoxysilane, $M_n = 1120 - 1250$ g/mol, Fluorochem). Unless specified, throughout the paper results for mPEG layers shown are for $mPEG_{9-12}$. Solvents used for the reactions were either isopropyl alcohol (IPA, 99.9 %, analytical grade) or ethanol (EtOH, 99.5 %, analytical grade). Initial synthesis of mPEG was done by immersion using toluene solutions (Merck analytical grade) and HCl (37%, Sigma-Aldrich), for the data in Figure 2. Washing solvents for the grafted layers were EtOH and toluene (Merck). H_2SO_4 (sulfuric acid, 97%, Merck) and acetic acid (glacial, Sigma-Aldrich) were used as catalysts. PDMS and mPEG solutions were spin coated under the conditions described in the text and in Supporting Information Table S1 (WS-400B-6NPP/LITE, Laurell).

4.2 Preparation of SCALS

4.2.1 Preparation of polymer solutions

When the mPEG layers were prepared by immersion in solution, clean silicon wafers were immersed in a solution containing 1 µL of mPEG, 8 µL of 37 % HCl, and 10 mL of anhydrous toluene and placed within a sealed and N_2-purged Atmosbag to react for 18 hours at room temperature, following a published protocol.[8] The coated substrates were thoroughly rinsed by immersion and agitation (1 minute) in anhydrous toluene, ethanol, and Milli-Q water, then immediately stored in Milli-Q water.

When the mPEG layers were prepared by drop casting, the silicon wafers were immersed

in a solution of ≈ 7 wt% mPEG in a 95/5/2 EtOH/water/AA wt% solvent mixture, which was pH adjusted to 4 using glacial acetic acid (AA) prior to the addition of the polymer. The solution was allowed to hydrolyze for 2 hours prior to use.

Given the low CAH achieved by spin coating, most of the work in this study was performed on surfaces prepared by spin coating. When SCALS were prepared by spin coating, a dilute solution of either PDMS (Table 2), mPEG (Table 1) or a mixture of the two (Table S5) was used. The starting point for the PDMS reaction conditions came from the work of Wang and McCarthy[15], while the mPEG reaction was inspired by the work of Katselas[42] and Papra et al.[8]. Silanol formation and stability is known to be affected by solution pH, choice of solvent, and water content.[43] Isopropyl alcohol (IPA) and ethanol (EtOH) were used as solvents as they are non-toxic, and they dissolve both low-MW OH-PDMS and mPEG (the mixture of PDMS and mPEG is compatible with IPA, Table S4); low amounts of H_2SO_4 and acetic acid were used as catalysts, and the individual role of each was tested. These reaction solutions were prepared in ambient lab conditions (22 °C and 65 % RH), and are stable for multiple weeks[15,22]. The reaction only commences once the solvent evaporates during spin coating; during this period relative humidity must be controlled[15,22].

Extensive optimization of the choice of catalyst and solvents was performed, as demonstrated in Section S2. Silane polymerization (both the hydrolysis and condensation reactions, Figure 1d)- f)) proceeds very slowly in the absence of a catalyst due to the limited reactivity of silane monomers. Various catalysts, including mineral acids, organic acid (e.g., HCl, acetic acid) and organometallic compounds (e.g., dibutyltin dilaurate), significantly enhance the reaction rate. The use of these catalysts not only improves the speed of polymerization but also influences the structural properties of the resulting polymers, making them essential for industrial applications.[44] For spin coating of mPEG, 95 wt% of ethanol and 5 wt% of Milli-Q water were thoroughly mixed and adjusted to pH = 4 adding acetic acid (2 wt%).

4.2.2 Cleaning of silicon substrates

Silicon wafers (prime grade, Micro Materials) were cut into 15 mm × 15 mm pieces and were extensively cleaned prior to grafting, using sonication in Milli-Q water, ethanol, and acetone for 1 min each, CO_2 snow jet cleaning on a hot plate at 150 °C, and 10 min of air plasma treatment (0.6 bar, 45 W, Harrick Plasma). The plasma treatment activates the silicon oxide native layer, creating additional surface silanol groups that react with the silanol groups in the reactive species.

4.2.3 Grafting of layers

Three synthesis methods were initially tested for mPEG solutions: i) by immersion using toluene solutions for 18 hours (as described above, the results are shown in Figure 2), based on a published immersion protocol;[8] ii) drop casting of toluene solutions, in which the polymer solution was dropped onto the substrate and left to dry over 15 minutes (results shown in Figure 2); iii) spin coating of ethanol solutions or IPA solutions (used throughout the paper).

In spin coating, after cleaning the substrate and before spin coating, the substrates were pre-heated at 150 °C for 1 min to reduce the amount of bound water; they were then moved to the spin coater chamber which was filled with high purity nitrogen, and spin coating was only initiated once the relative humidity (RH) reached below 10% (measured using a Lutron HT-305 probe inserted into the spin-coating chamber). Some grafting tests were done in absence of humidity control, but the results were not reproducible even when the RH was supposedly unchanged, as shown in Table S2. Spin coating was performed for 65 s, in the conditions shown in Table 1 and Table 2. The reactant solution was applied 5 s after the spin coater started (i.e., once the substrate was spinning at the target rpm), meaning the actual spin-coating time was 60 s. Longer spin-coating times did not enhance coating properties. To accelerate the grafting reaction, after spin coating a post-cure step was used (heating in an oven at set temperature and time). The hydrolysis and condensation reactions involved in silane polymerization are endothermic, so increasing the temperature enhances the rate of

silane polymerization.[44] Finally, to remove physisorbed polymers, the layers were submerged in toluene and ethanol and agitated for 1 min each, then blown dry with nitrogen and stored in air for characterization.

4.3 Layer characterization

4.3.1 Thickness Measurements

All prepared layers were characterized by spectroscopic ellipsometry (M2000, J.A. Woollam), in a lab with RH$\approx 60-70\%$. Measurements were taken at 600 wavelengths equally spaced between 370 and 1000 nm, at a single angle of incidence of 70°. Data were analyzed in CompleteEASE with a model consisting of a silicon backing layer, a silica native oxide layer (thickness fixed at 1.9 nm), and a PDMS or mPEG layer defined by a Cauchy model (PDMS $A = 1.4,\ B = 0.005,\ C = 0$; mPEG: $A = 1.3,\ B = 0.05,\ C = 0$), the thickness of which was allowed to vary. For mixed layers the refractive index was assumed to be the average of the refractive index of PDMS and of mPEG. Specular neutron reflectometry (NR) measurements were conducted on the *Platypus* time-of-flight reflectometer at the Australian Centre for Neutron Scattering, ANSTO. NR was measured as a function of the scattering vector, $Q = (4\pi/\lambda)sin\theta$, where λ is the wavelength and θ is the angle of incidence. Measurements were made on the mPEG layers in air and against liquid D_2O, and more details are shown in Section S4. NR data in Figure S5 show that the thickness of mPEG layers taken at $\approx 0\%$ RH increased by about 1 nm when the measurements were taken in RH$\approx 100\%$, and by 2 nm when immersed in water.

4.3.2 Contact Angle Goniometry

The advancing and receding contact angle were measured using a KSV CAM200 goniometer by slowly increasing and reducing the volume of a probe water drop. A custom translation stage was fitted to the goniometer that allowed for automated sample changing, and the software was modified to allow for the following recipe to be precisely followed. The protocol

was developed based on the principles of Huhtamaki et al.[45] and the work of Barrio-Zhang et al.[22] Initially, a 8 µL droplet of Milli-Q water was injected, and then the volume was increased to 16 µL at a rate of 0.05 µL s^{-1} and the advancing contact angle was measured. 10 µL was then added to and removed from the droplet at 0.5 µL s^{-1} to ensure the RCA was reached. Subsequently, the droplet volume was reduced a rate of 0.05 µL s^{-1} and the receding contact angle was measured before the contact line moved (1 image/s). The advancing and receding contact angle were both recorded for droplet volume of 12 ± 1 µL during the dispensing and withdrawing of water, respectively. ACA and RCA were taken as the average of 12 data points, CAH was taken as the difference between ACA and RCA. The average contact angle (CA) is the average of the ACA and the RCA.

4.3.3 Roll-Off Angle

Roll-off angles were measured using a custom-built setup. A 10 µL droplet was placed onto the coated substrate, and the substrate was tilted at a rate of 0.05 ° s^{-1} while recording a video. The angle at which the droplet began to slide was measured using Image J. In the Tables, errors correspond to the standard deviation of the mean. When no error is shown, only one repetition was conducted. All the plots display measurements on individual samples.

4.3.4 Atomic Force Microscopy

Sample topography, adhesion maps and meniscus force maps were measured using atomic force microscopy (AFM, Bruker Multimode 8) in PeakForce mode. Maps of maximum adhesion force were used to detect any evidence of microphase separation (indicated by nanoscale contrast in the micrographs) on the mixed SCALS system. Peakforce mode was used to collect meniscus force mapping (MFM, analyzed with a custom script), which revealed the topography and thickness of the liquid-like layers, as recently demonstrated by the authors.[18,34]

In each MFM map, 65,536 force curves were collected over a sample area and the attrac-

tion between the tip and a liquid film, due to capillary forces, measured at each point; on grafted layers, a film thickness higher than that due to a thin water layer adsorbed on the surface is obtained. The jump-in point (the position at which the AFM tip is attracted by the liquid meniscus) is used to extract layer thickness, and the position of the hard repulsion is used to reconstruct the substrate topography. The maximum adhesion force experienced by the tip when being withdrawn from the surface can be used to distinguish areas of different surface chemistry[23]. MFM is superior to conventional tapping-mode AFM as it makes it easier to track the liquid layer, and allows for simultaneous imaging of adhesion, substrate topography, and layer thickness. PeakForce scans were conducted using Bruker FMV-A tips (spring constant $\approx 3\,\mathrm{N\,m^{-1}}$) with an image size of 500 nm, resolution of 256×256, scan rate of 1.0 Hz, peak force of 5 nN, and amplitude of $\approx$30 nm. The spring constant was determined through thermal tuning. Data were processed and converted into images of substrate topography and jump-in location using the code documented by Rasera et al.[18].

5 Supporting Information

Additional information is provided in the attached pdf document:

S1 Further details regarding individual PDMS and mPEG reaction conditions, including additional AFM images

S2 Further details regarding mixed PDMS and mPEG reaction conditions

S3 Further details regarding the two-step procedure for producing mixed mixed PDMS/mPEG layers

S4 Neutron reflectometry characterization of layer thickness, including the effect of relative humidity on mPEG layer thickness.

S5 Comparison of the results in Figure 5 to those of Lepikko et al.

6 Acknowledgments

The authors acknowledge funding from the Australian Research Council (FT180100214 and DP230100555). Dr Andrew Nelson is acknowledged for help in collecting neutron reflectometry data.

References

(1) Gresham, I. J.; Neto, C. Advances and challenges in slippery covalently-attached liquid surfaces. *Adv. Colloid Interface Sci.* **2023**, *315*, 102906.

(2) Chen, L.; Huang, S.; Ras, R. H. A.; Tian, X. Omniphobic liquid-like surfaces. *Nat. Rev. Chem.* **2023**, *7*, 123–137.

(3) Gresham, I. J.; Lilley, S. G.; Nelson, A. R. J.; Koynov, K.; Neto, C. Nanostructure Explains the Behavior of Slippery Covalently Attached Liquid Surfaces. *Angew. Chem. Int. Ed.* **2023**, *62*, e202308008.

(4) Eduok, U.; Faye, O.; Szpunar, J. Recent developments and applications of protective silicone coatings: A review of PDMS functional materials. *Prog. Org. Coat.* **2017**, *111*, 124–163.

(5) Khan, M. U. A.; Aslam, M. A.; Bin Abdullah, M. F.; Hasan, A.; Shah, S. A.; Stojanović, G. M. Recent perspective of polymeric biomaterial in tissue engineering– a review. *Mater. Today Chem.* **2023**, *34*, 101818.

(6) Kingshott, P.; Griesser, H. J. Surfaces that resist bioadhesion. *Curr. Opin. Solid State Mater. Sci.* **1999**, *4*, 403–412.

(7) Jo, S.; Park, K. Surface modification using silanated poly(ethylene glycol)s. *Biomater.* **2000**, *21*, 605–616.

(8) Papra, A.; Gadegaard, N.; Larsen, N. B. Characterization of Ultrathin Poly(ethylene glycol) Monolayers on Silicon Substrates. *Langmuir* **2001**, *17*, 1457–1460.

(9) Cha, H.; Vahabi, H.; Wu, A.; Chavan, S.; Kim, M.-K.; Sett, S.; Bosch, S. A.; Wang, W.; Kota, A. K.; Miljkovic, N. Dropwise condensation on solid hydrophilic surfaces. *Sci. Adv.* **2020**, *6*, eaax0746.

(10) Katselas, A.; Gresham, I. J.; Nelson, A. R. J.; Neto, C. Exploring the water capture efficiency of covalently attached liquid-like surfaces. *J. Chem. Phys.* **2023**, *158*, 214708.

(11) Boylan, D.; Monga, D.; Shan, L.; Guo, Z.; Dai, X. Pushing the Limit of Beetle-Inspired Condensation on Biphilic Quasi-Liquid Surfaces. *Adv. Funct. Mater.* **2023**, *33*, 2211113.

(12) Shabanian, S.; Zhao, X.; Au, S.; Furtak, N. T.; Golovin, K. Sustainable design of non-fluorinated yet oleophobic fibrous surfaces. *Journal of Materials Chemistry A* **2024**, *12*, 15716–15730.

(13) Butt, H.-J.; Liu, J.; Koynov, K.; Straub, B.; Hinduja, C.; Roismann, I.; Berger, R.; Li, X.; Vollmer, D.; Steffen, W.; Kappl, M. Contact angle hysteresis. *Curr. Opin. Colloid Interface Sci.* **2022**, *59*, 101574.

(14) McHale, G.; Gao, N.; Wells, G. G.; Barrio-Zhang, H.; Ledesma-Aguilar, R. Friction Coefficients for Droplets on Solids: The Liquid–Solid Amontons' Laws. *Langmuir* **2022**, *38*, 4425–4433.

(15) Wang, L.; McCarthy, T. J. Covalently Attached Liquids: Instant Omniphobic Surfaces with Unprecedented Repellency. *Angew. Chem. Int. Ed.* **2016**, *55*, 244–248.

(16) Khatir, B.; Azimi Dijvejin, Z.; Serles, P.; Filleter, T.; Golovin, K. Molecularly Capped Omniphobic Polydimethylsiloxane Brushes with Ultra-Fast Contact Line Dynamics. *Small* **2023**, *19*, 2301142.

(17) Lepikko, S.; Jaques, Y. M.; Junaid, M.; Backholm, M.; Lahtinen, J.; Julin, J.; Jokinen, V.; Sajavaara, T.; Sammalkorpi, M.; Foster, A. S.; Ras, R. H. A. Droplet slipperiness despite surface heterogeneity at molecular scale. *Nat. Chem.* **2024**, *16*, 506–513.

(18) Rasera, F.; Gresham, I. J.; Tinti, A.; Neto, C.; Giacomello, A. Molecular Origin of Slippery Behavior in Tethered Liquid Layers. *ACS Nano* **2025**, *19*, 8020–8029.

(19) Zhou, X.; Wang, Y.; Li, X.; Sudersan, P.; Amann-Winkel, K.; Koynov, K.; Nagata, Y.; Berger, R.; Butt, H. J. Thickness of Nanoscale Poly(Dimethylsiloxane) Layers Determines the Motion of Sliding Water Drops. *Adv. Mater.* **2024**, e2311470.

(20) Golovin, K. Design and Application of Surfaces with Tunable Adhesion to Liquids and Solids. 2017; PhD Thesis, Chapter 5.

(21) Giacomello, A.; Schimmele, L.; Dietrich, S. Wetting hysteresis induced by nanodefects. *Proc Natl Acad Sci U S A* **2016**, *113*, E262–71.

(22) Barrio-Zhang, H.; Ruiz-Gutiérrez, E.; Armstrong, S.; McHale, G.; Wells, G. G.; Ledesma-Aguilar, R. Contact-Angle Hysteresis and Contact-Line Friction on Slippery Liquid-like Surfaces. *Langmuir* **2020**, *36*, 15094–15101.

(23) Becher-Nienhaus, B.; Liu, G.; Archer, R. J.; Hozumi, A. Surprising Lack of Influence on Water Droplet Motion by Hydrophilic Microdomains on Checkerboard-like Surfaces with Matched Contact Angle Hysteresis. *Langmuir* **2020**, *36*, 7835–7843.

(24) Prime, K. L.; Whitesides, G. M. Adsorption of proteins onto surfaces containing end-attached oligo(ethylene oxide): a model system using self-assembled monolayers. *J. Am. Chem. Soc.* **1993**, *115*, 10714–10721.

(25) Mrksich, M.; Whitesides, G. M. Using Self-Assembled Monolayers to Understand the Interactions of Man-made Surfaces with Proteins and Cells. *Annu. Rev. Biophys. Biomol. Struct.* **1996**, *25*, 55–78.

(26) Fadeev, A. Y.; McCarthy, T. J. Binary Monolayer Mixtures: Modification of Nanopores in Silicon-Supported Tris(trimethylsiloxy)silyl Monolayers. *Langmuir* **1999**, *15*, 7238–7243.

(27) Fadeev, A. Y.; McCarthy, T. J. Trialkylsilane Monolayers Covalently Attached to Silicon Surfaces: Wettability Studies Indicating that Molecular Topography Contributes to Contact Angle Hysteresis. *Langmuir* **1999**, *15*, 3759–3766.

(28) Overney, R. M.; Meyer, E.; Frommer, J.; Brodbeck, D.; Lüthi, R.; Howald, L.; Guntherodt, H. J.; Fujihira, M.; Takano, H.; Gotoh, Y. Friction measurements on phase-separated thin films with a modified atomic force microscope. *Nature* **1992**, *359*, 133–135.

(29) Folkers, J.; Laibinis, P.; Whitesides, G. Self-Assembled Monolayers of Alkanetiols on Gold: Comparisons of Monolayers Containing Mixtures of Short- and Long- Chain Contituents with CH3 and CH2OH Terminal Groups. *Langmuir* **1992**, *8*, 1330–1341.

(30) Laibinis, P. E.; Whitesides, G. M. Omega-Terminated alkanethiolate monolayers on surfaces of copper, silver, and gold have similar wettabilities. *J. Am. Chem. Soc.* **1992**, *114*, 1990–1995.

(31) Stranick, S. J.; Parikh, A. N.; Tao, Y. T.; Allara, D. L.; Weiss, P. S. Phase Separation of Mixed-Composition Self-Assembled Monolayers into Nanometer Scale Molecular Domains. *J. Phys. Chem.* **1994**, *98*, 7636–7646.

(32) Fadeev, A. Y.; McCarthy, T. J. Self-Assembly Is Not the Only Reaction Possible between Alkyltrichlorosilanes and Surfaces: Monomolecular and Oligomeric Covalently Attached Layers of Dichloro- and Trichloroalkylsilanes on Silicon. *Langmuir* **2000**, *16*, 7268–7274.

(33) Konku-Asase, Y.; Yaya, A.; Kan-Dapaah, K. Curing Temperature Effects on the Tensile

Properties and Hardness of γ–Fe2O3 Reinforced PDMS Nanocomposites. *Adv. Mater. Sci. Eng.* **2020**, *2020*, 562373.

(34) Peppou-Chapman, S.; Neto, C. Mapping Depletion of Lubricant Films on Antibiofouling Wrinkled Slippery Surfaces. *ACS Appl. Mater. Interfaces* **2018**, *10*, 33669–33677.

(35) James, M.; Darwish, T. A.; Ciampi, S.; Sylvester, S. O.; Zhang, Z.; Ng, A.; Gooding, J. J.; Hanley, T. L. Nanoscale condensation of water on self-assembled monolayers. *Soft Matter* **2011**, *7*, 5309.

(36) Cassie, A. B. D. Contact angles. *Discuss. Faraday Soc.* **1948**, *3*, 11–16.

(37) Reyssat, M.; Quéré, D. Contact Angle Hysteresis Generated by Strong Dilute Defects. *J. Phys. Chem. B* **2009**, *113*, 3906–3909, 27.

(38) Adamson, A.; Gast, A. *Physical Chemistry of Surfaces*, 6th ed.; Wiley-Blackwell: New York, 1997.

(39) Extrand, C. W. Contact Angles and Hysteresis on Surfaces with Chemically Heterogeneous Islands. *Langmuir* **2003**, *19*, 3793–3796.

(40) Joanny, J. F.; de Gennes, P. G. A model for contact angle hysteresis. *J. Chem. Phys.* **1984**, *81*, 552–562.

(41) Oesterhelt, F.; Rief, M.; Gaub, H. E. Single molecule force spectroscopy by AFM indicates helical structure of poly(ethylene-glycol) in water. *New J. Phys.* **1999**, *1*, 6.

(42) Katselas, A. Nanoscale Coatings for the Enhancement of Atmospheric Water Capture. PhD Thesis, University of Sydney, 2024; `https://hdl.handle.net/2123/32268`.

(43) Pantoja, M.; Díaz-Benito, B.; Velasco, F.; Abenojar, J.; del Real, J. C. Analysis of hydrolysis process of γ-methacryloxypropyltrimethoxysilane and its influence on the formation of silane coatings on 6063 aluminum alloy. *Appl. Surf. Sci.* **2009**, *255*, 6386–6390.

(44) Issa, A.; Luyt, A. Kinetics of Alkoxysilanes and Organoalkoxysilanes Polymerization: A Review. *Polymers* **2019**, *11*, 537.

(45) Huhtamaki, T.; Tian, X.; Korhonen, J. T.; Ras, R. H. A. Surface-wetting characterization using contact-angle measurements. *Nat Protoc* **2018**, *13*, 1521–1538.

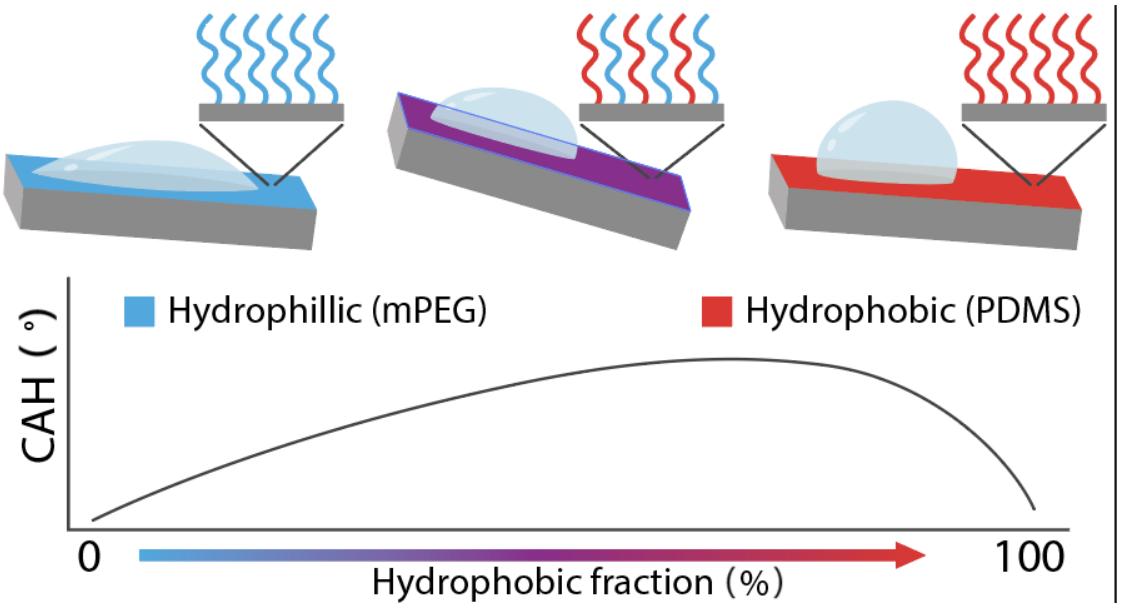
Hydrophillic (mPEG)
Hydrophobic (PDMS)
CAH (°)
0
100
Hydrophobic fraction (%)